Anticancer drug delivery system based on calcium carbonate particles loaded with a photosensitizers.

Yulia Svenskaya[a,b], Bogdan Parakhonskiy[a,c,*], Albrecht Haase[d], Vsevolod Atkin[b], Evgeny Lukyanets[e], Dmitry Gorin[b], and Renzo Antolini[d]

a) BIOtech Center Dept. of Industrial Engineering, University of Trento,via delle Regole 101, 38123 Mattarello, Italy
b) Saratov State University, Astrakhanskaya street 83, 410012, Saratov, Russia
c) A.V. Shubnikov Institute of Crystallography Russian Academy of Science, Leninskiy prospect 59, 119333, Moscow, Russia
d) Department of Physics, University of Trento, via Sommarive 14, 38123 Povo, Italy
e) Organic Intermediates and Dyes Institute, B. Sadovaya 114, 123995, Moscow, Russia
*corresponding author: bogdan.parakhonskiy@unitn.it

Highlights

- Vaterite particles were loaded with the photosensitizer Photosens used in PDT
- The drug release process was triggered by a $CaCO_3$ crystal phase transition
- Release dynamics were found to be sensitive to the environmental pH
- The phase transition speeds up with increasing particle size
- This allows to create a controllable photosensitizer delivery system, releasing its payload under acidy conditions

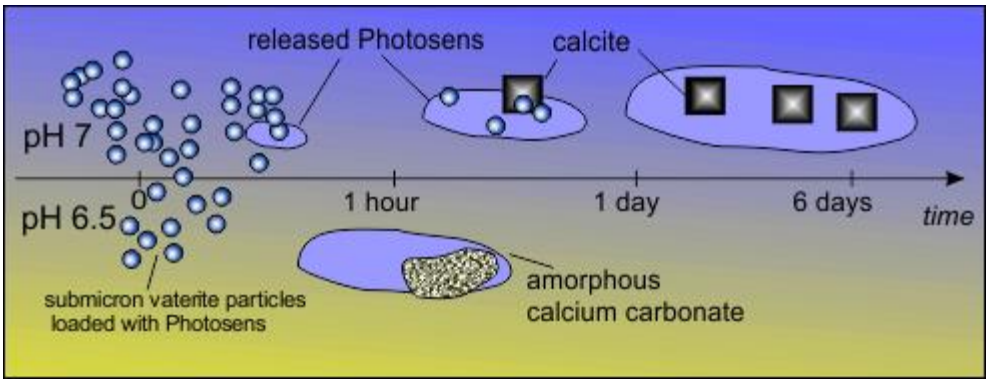

Abstract

In photodynamic therapy (PDT), photosensitizers are required to arrive in high concentrations at selective targets like cancer cells avoiding toxicity in healthy tissue. In this work, we propose the application of porous calcium carbonate carriers in the form of polycrystalline vaterite for this task. We investigated the loading efficiency for the photosensitizer Photosens in micrometer- and sub-micrometer-sized vaterite carriers. A possible release mechanism dependening on the surrounding

pH was studied, showing a fast degradation of the carriers in buffers below pH 7. These results hold out the prospect of a novel PDT drug delivery system. Variation of particle size or additional coatings allow to custom-design workload release curves. An intrinsic cancer-sensitivity can be expected from the pH-dependent release in the acidic microenvironment of cancer tissue.

Keywords

calcium carbonate, vaterite, photosens, drug delivery, cancer**,** phthalocyanine

1 Introduction

One of the major challenge in nanomedicine is the development of systems for targeted substance delivery, which requires understanding of fundamental biochemical processes such as cellular uptake mechanisms [1,2] or intracellular transport [3], but also the intelligent design of adequate carriers [4–6]. An effective matrix for such a delivery system is calcium carbonate ($CaCO_3$) [10–13]. $CaCO_3$ exists in three different anhydrous crystalline polymorphs: calcite, aragonite, and vaterite. Under standard conditions for temperature and pressure, calcite is the stable phase, while aragonite and vaterite are metastable forms that readily transform into the stable phase. Vaterite is an ideal candidate for a drug delivery system because it has large porosity, large surface area, and can decompose rapidly under relatively mild conditions [10,11]. Vaterite is the least stable phase of $CaCO_3$ since in contact with water it slowly dissolves and recrystallizes to form calcite. Previous studies described the possibility of synthesizing spherical mono-dispersed vaterite particles in the size range from 2 to 10 µm [11] and from 400 nm to 2.4 µm [12]. Vaterite containers allow for different substance loading methods such as adsorption [13–15] and co-precipitation [8,14]. A release mechanism based on a crystal phase transition has recently been demonstrated [12,15,16]. Cytotoxicity and influence on cell viability have been excluded in cell culture studies with 400 nm vaterite containers. Apart from this efficient cellular uptake of substance-loaded containers was observerd [15].

To exploit vaterite containers as a drug delivery system in photodynamic therapy (PDT), photosensitizers have to be incorporated, delivered to the target, and released within the cells. Exposure to light at the photosensitizers absorbance wavelength then induces singlet oxygen generation, a photochemical reaction of type II [17,18]. The singlet oxygen can oxidize cellular macromolecules like lipids, nucleic acids, and amino acids leading to cancer cell apoptosis [19].

So far, the main negative side effect of PDT is caused by its insufficient selectivity of action: a high concentration of photosensitizer is required for cancer treatment at the tumour site, but causes incidental toxicity in healthy tissue. This side effect could be strongly reduced by targeted delivery to the region of interest. The proposed delivery system will achieve this exploiting a pH-dependency of the carrier degradation dynamics.

2 Materials and Methods

2.1 Materials

Calcium chloride, sodium carbonate, and acetate were purchased from Sigma-Aldrich and used without further purification. The photosensitizer Photosens, a mixture of sulfonated aluminum phthalocyanines $AlPcS_n$, with n = 2, 3 or 4 (the mean n = 3.1), was obtained from the Organic Intermediates and Dyes Institute (Moscow, Russia). It has strong absorption bands with a maximum at 675 nm wavelength [20], and can be activated at 100 J/cm^2 light power [21]. It is applied in clinical practice since 2001 (Registration Certificate Ministry of Health of Russian Federation № 000199.01-2001) in both diagnostics [22,23] and treatment, from of lip, pharynx, larynx, and tongue lesions to lung and esophageal tumour therapy [24–26].

2.2 Particle preparation and characterization

Spheroid-like calcium carbonate microparticles of 3.6±0.5 μm size were fabricated using a previously reported protocol [10]: 1 mL of Na_2CO_3 (0.33 M) was loaded into a glass vessel, then an equal volume of $CaCl_2$ (0.33 M) was added and stirred at 500 rpm for 1 min. For the preparation of sub-micron vaterite spheres with a size 650±30 nm, the protocol described in [12] was applied: the chosen concentrations of $CaCl_2$ and Na_2CO_3 were 0.33 M. Ethylene glycol (EG) was added to this reaction solution (Na_2CO_3 and $CaCl_2$ were dissolved each in 2 ml water and 10 ml EG). The solution was stirred with 500 rpm at room temperature for 3 h. The mixed solution turned opaque almost instantly. The synthesized $CaCO_3$ particles were carefully washed with ethanol and dried for 30 min at 60°C.

The drug Photosens was loaded into the obtained vaterite containers by the adsorption method: 5 mg of dried $CaCO_3$ particles were taken for each sample, 1.5 ml of 0.5 mg/ml aqueous solution of the drug were added. The adsorption took place during 2.5 h of shaking. Micron-sized particles were centrifuged at 3200×g for 1 min, sub-micron particles for 3 min. Afterwards the supernatants were removed and collected.

To study the morphology and microstructure, dried particles were sputtered with gold and imaged with a scanning electron microscopes (SEM), a MIRA II LMU (Tescan) at an operating voltage of 20 kV and a Phillips XL 30 at 5-30 keV.

2.3 Loading and release process

Optical studies of the loading process were performed using a two-photon laser scanning microscope Ultima IV (Prairie Technologies) with a 100× objective (NA 1.0, water immersion, Olympus) and an ultra-short pulsed laser (Mai Tai Deep See HP, Spectra-Physics) at an excitation wavelength of 800 nm.

A spectrofluorometer (Cary Eclipse, Varian) was used to measure the Photosens uptake efficiency and release profile. The weight of the particle samples was kept constant (5 mg) in all experiments. Some loss of containers during the washing may have occurred, but did not exceed a few percent. As a measure of the amount of Photosens in solution, its fluorescence intensity was recorded at 684 nm. A calibration curve was obtained from fluorescence measurements of known concentrations of Photosens. Then samples were diluted in water or buffer solution to ensure that

measurements were within the linear range of the calibration curve. The total amount of adsorbed molecules was deduced by subtracting the measured amount of unloaded and washed-off molecules of the supernatant from the initial amount of 0.5 mg/ml of Photosens, which had been added to the system.

To study the release of the drug under varying pH, a line of acetate buffers from pH 4.5 to pH 7 was created. Vaterite containers loaded with Photosens were suspended in these buffers (5 mg particles in 30 ml) and incubated at room temperature in carefully sealed centrifuge tubes. After different incubation times (5 min to 6 days), the samples were centrifuged at 2600×g for 3 min and the concentration of the released Photosens in the supernatant was measured by spectrofluorimetry.

To study the calcium carbonate phase change during the release process, samples were monitored by SEM. Samples were dried from 10 μl of particle suspension Based on SEM image analysis, the calcium carbonate phases were determinate via their specific properties: vaterite being spherical and polycrystalline (Fig. 1), calcite being a rhombohedral monocrystal (Fig. 2 A), and amorphous calcium carbonate showing up as non-regular structures with grain sizes less than 20 nm (Fig. 2 C, D).

3 Results and discussions

3.1 Particle loading

To study the influence of the carrier size on the loading efficiency, two lines of the vaterite particles were synthesized: vaterite containers with an average size of 650±30 nm (hereafter referred to as "small") and of size 3.6±0.5 μm (hereafter referred to as "big"). In 5 mg of small particles 0.067±0.007 mg of Photosens could be incorporated, which amounts to 1.4±0.4% (w/w). For big particles the uptake was 0.047±0.003 mg, corresponding to 0.9±0.2% (w/w). The loading efficiencies of big and small particles are comparable which proves a deep internalization of the drug into the calcium carbonate matrix, a factor of 6 between small and big particle loading would reflect an adsorption only to the external surface. These efficiencies are in the same order as those of other substances loaded via adsorption into porous carriers [8,27,28]. Scanning electron microscopy images and two-photon fluorescent images of the loaded particles are presented in Fig. 1. The SEM images in Fig. 1A and 1B show the spherical shape of the vaterite polycrystals and their narrow size dispersion. The fluorescence signals from two-photon microscopy in Fig. 1C and 1D show that particles were successfully loaded with the drug Photosens, preserving its fluorescence properties.

Fig. 1

3.2 Release process

The release of the payload from the porous particles is an interplay of drug desorption and carrier dissolution [29]. In the absence of a payload-specific solvent, the process of desorption of the

loaded drug from the carriers is usually very slow, but increases when the carriers size decreases. Desorption is strongly enhanced if a suitable solvent penetrates into the carrier and dissolves the drug, which then diffuses faster out into the medium. This is the case for Photosens loaded particles dispersed in a water-based solution.

Furthermore, the carriers themselves can be degraded or dissolved by the surrounding medium, causing the payload to diffuse from the carrier. This process sets in if the carriers are metastable as in the case of vaterite in water. The dominance of drug desorption or carrier degradation is strongly dependent on the immersion medium properties and can be studied by monitoring the payload release time curves.

During the desorption-adsorption process, phthalocyanine molecules get detached and reattached until a dynamic equilibrium is reached, causing small modulations in the release curve. When the particle dissolution sets in, the release is enhanced and reaches 100% when all carries are dissolved. Depending on the immersion medium, the vaterite particles dissolve or a crystal phase transition sets in, where the external layer of vaterite starts to ionize, seeding the formation of calcite monocrystals from the ions. Typical SEM images of these phases are shown in Fig. 2.

Fig. 2

The release curves of Photosens from vaterite containers were monitored via spectrofluorimetry and the corresponding calcium carbonate crystal phases via SEM for both carrier sizes. Observations started 5 min after immersion and lasted up to 6 days. In different experimental series the pH of the immersion medium was varied.

The results of the SEM image analysis are graphically summarized in Fig. 3, where the presences of the three phases that are a relevant to the release states of Photosens is shown as a function of incubation time and solution pH. The marked phase transitions are approximated conditions under which new phases appear. While Photosens is confined within the vaterite particles, it gets released during the transition to calcite or amorphous calcium carbonate except for residual amounts of the drug which reattach to the external surfaces.

Exemplary SEM images for all points of this phase diagram can be found in the supplementary material (Fig. S1 and Fig. S2).

The outstanding result of this analysis is the global tendency of particles to dissolve rapidly with decreasing pH, forming calcite crystals and/or amorphous $CaCO_3$. This reflects the increasing solubility of calcium carbonate with decreasing pH, and the relative difference in solubility by a factor of 3.7 between vaterite and calcite [30].

Fig. 3

At neutral pH=7, a clear decrease of the dissolution timescale with increasing carrier size was observed, the mechanism is a phase transition from vaterite to calcite (see Fig. 3 and Fig. 2B). The

transition sets in at around 24 h for both type of particles and is completed after day 3 for big particles and after day 6 for small particles.
With increasing acidity, the carrier dissolution times decrease and an amorphous phase (Fig. 3 and Fig. 2C, D) was found either before the recrystallization to calcite or as final state. The time until the vaterite crystals vanish completely decreases strongly with decreasing pH, so the drug release is governed more and more by the dissolution of the carriers.
At intermediate acidity of pH 6.5 to 5, the dissolution times keep shortening, vaterite particles dissolve completely within the first day. The fastest phase transition was observed at very low pH of 5 to 4.5, where both sizes of vaterite particles dissolved within the first 5 min causing an immediate burst release of the drug.

Fig. 4.

The measured payload release curves in neutral buffers are presented in Fig. 4.
The processes can be interpreted in the following way: drug release is governed first by desorption and then followed by a complete release during the phase transition. In our experiment a partial re-adsorption of the phthalocyanine molecules to the newly formed crystal structures was observed, which limits the released amount. Instead in the open environment of a drug delivery application, a complete dispersion of the loaded substance can be expected after the dissolution of the vaterite particles. The differences between the curves of big and small particles are of two kinds, the time until the release saturates increased from 1 to 4 days, and the saturation level is lower for big particles because of an enhanced re-adsorption due to more effective re-attachment to newly formed calcite structures.
Decreasing the carrier size leads in all buffer solutions to a prolongation of the release time, this effect could be further enhanced by additional coatings [13]. Also tumour selectivity could be obtained through a particle surface modification, e.g by attaching ligands interacting preferentially or specifically with tumour cells like monoclonal antibodies [31–33].

Another advantage of the sub-micron carriers is the fact that in buffers below pH 7 they dissolve completely into the fully degradable amorphous phase.
This pH-dependence opens up new possibilities for targeted delivery, since the microenvironment in tumors is generally more acidic than in normal tissues [34]. During endocytosis via the endosomal-lysosomal degradation pathway, the pH level drops in the endocytotic vesicles to 5.0 with respect to 7.4 in the cytoplasma. This would trigger an immediate release of the loaded substance. Since this acidic pH in these vesicles is maintained by an energy-consuming proton pump, this release would be selective to viable cancer cells [35].
The pH-sensitivity may thus delay drug release from containers in the bloodstream (pH=7.4) and concentrate it to the intracellular compartments of targeted cancer cells.
In conclusion, this opens up the perspective of a novel drug delivery system based on porous calcium carbonate carriers. Modification of particle size and pH will allow to customize the

workload release curves. A drug delivery system with pH-controlled release promises intracellular delivery with a high selectivity to cancer cells. In combination with an otherwise poorly selective photosensitizer this could become a strong cancer-therapeutic tool, where the carrier degradability could be tuned to control the rate of drug release [36].

[1] L.M. Bareford, P.W. Swaan, Endocytic mechanisms for targeted drug delivery., Adv. Drug Delivery Rev. 59 (2007) 748–58.

[2] J. Rejman, V. Oberle, I.S. Zuhorn, D. Hoekstra, Size-dependent internalization of particles via the pathways of clathrin- and caveolae-mediated endocytosis., Biochem. J. 377 (2004) 159–69.

[3] T.-G. Iversen, T. Skotland, K. Sandvig, Endocytosis and intracellular transport of nanoparticles: Present knowledge and need for future studies, Nano Today. 6 (2011) 176–185.

[4] D.A. Edwards, J. Hanes, G. Caponetti, J. Hrkach, A. Ben-Jebria, M.L. Eskew, et al., Large porous particles for pulmonary drug delivery., Science. 276 (1997) 1868–71.

[5] M. Kester, Y. Heakal, T. Fox, A. Sharma, G.P. Robertson, T.T. Morgan, et al., Calcium phosphate nanocomposite particles for in vitro imaging and encapsulated chemotherapeutic drug delivery to cancer cells., Nano Lett. 8 (2008) 4116–21.

[6] P. Couvreur, C. Vauthier, Nanotechnology: intelligent design to treat complex disease., Pharm. Res. 23 (2006) 1417–50.

[7] D. V. Volodkin, N.I. Larionova, G.B. Sukhorukov, Protein encapsulation via porous CaCO3 microparticles templating., Biomacromolecules. 5 (2004) 1962–72.

[8] A.I. Petrov, D. V. Volodkin, G.B. Sukhorukov, Protein-calcium carbonate coprecipitation: a tool for protein encapsulation., Biotechnology Progress. 21 (2005) 918–25.

[9] D. V Volodkin, R. von Klitzing, H. Möhwald, Pure protein microspheres by calcium carbonate templating., Angew. Chem., Int. Ed. Engl. 49 (2010) 9258–61.

[10] D. V Volodkin, A.I. Petrov, M. Prevot, G.B. Sukhorukov, Matrix Polyelectrolyte Microcapsules: New System for Macromolecule Encapsulation, Langmuir. 20 (2004) 3398–3406.

[11] S. Schmidt, D. Volodkin, Microparticulate biomolecules by mild CaCO3 templating, J. Mater. Chem. B. 1 (2013) 1210.

[12] B. V. Parakhonskiy, A. Haase, R. Antolini, Sub-Micrometer Vaterite Containers: Synthesis, Substance Loading, and Release, Angew. Chem., Int. Ed. Engl. 51 (2012) 1195–1197.

[13] C. Peng, Q. Zhao, C. Gao, Sustained delivery of doxorubicin by porous CaCO3 and chitosan/alginate multilayers-coated CaCO3 microparticles, Colloids Surf., A. 353 (2010) 132–139.

[14] Z. She, M.N. Antipina, J. Li, G.B. Sukhorukov, Mechanism of protein release from polyelectrolyte multilayer microcapsules., Biomacromolecules. 11 (2010) 1241–1247.

[15] B. V. Parakhonsky, C. Foss, E. Carletti, M. Fedel, A. Haase, A. Motta, et al., Tailored intracellular delivery via a crystal phase transition in 400 nm vaterite particles, Biomaterials Science. (2013).

[16] B. V. Parakhonskiy, F. Tessarolo, A. Haase, R. Antolini, Dependence of Sub-Micron Vaterite Container Release Properties on pH and Ionic Strength of the Surrounding Solution, Advances in Science and Technology. 86 (2012) 81–85.

[17] M. DeRosa, R. Crutchley, Photosensitized singlet oxygen and its applications, Coord. Chem. Rev. 233-234 (2002) 351–371.

[18] E.A. Lukyanets, Phthalocyanines as Photosensitizers in the Photodynamic Therapy of Cancer, J. Porphyrins Phthalocyanines. 03 (1999) 424–432.

[19] H. Guo, H. Qian, N.M. Idris, Y. Zhang, Singlet oxygen-induced apoptosis of cancer cells using upconversion fluorescent nanoparticles as a carrier of photosensitizer., Nanomedicine. 6 (2010) 486–95.

[20] O.I. Trushina, E.G. Novikova, V. V Sokolov, E. V Filonenko, V.I. Chissov, G.N. Vorozhtsov, Photodynamic therapy of virus-associated precancer and early stages cancer of cervix uteri., Photodiagnosis and Photodynamic Therapy. 5 (2008) 256–9.

[21] R.R. Allison, G.H. Downie, R. Cuenca, X.-H. Hu, C.J. Childs, C.H. Sibata, Photosensitizers in clinical PDT, Photodiagn. Photodyn. Ther. 1 (2004) 27–42.

[22] S.A. Shevchik, M. V Loshchenov, G.A. Meerovich, M. V Budzinskaia, N.A. Ermakova, S.S. Kharnas, et al., A device for fluorescence diagnosis and photodynamic therapy of eye diseases, by using photosense., Vestnik Oftalmologii. 121 (n.d.) 26–8.

[23] M. V Budzinskaia, S.A. Shevchik, T.N. Kiseleva, V.B. Loshchenov, I. V Gurova, I. V Shchegoleva, et al., Role of fluorescence diagnosis using Photosens in patients with subretinal neovascular membrane., Vestnik Oftalmologii. 123 (2007) 11–6.

[24] L. V Uspenskiĭ, L. V Chistov, E.A. Kogan, V.B. Loshchenov, I. Ablitsov, V.K. Rybin, et al., Endobronchial laser therapy in complex preoperative preparation of patients with lung diseases, Khirurgiia. (2000) 38–40.

[25] E.F. Stranadko, M.I. Garbuzov, V.G. Zenger, A.N. Nasedkin, N.A. Markichev, M. V Riabov, et al., [Photodynamic therapy of recurrent and residual oropharyngeal and laryngeal tumors]., Vestnik Otorinolaringologii. 38 (2001) 36–9.

[26] E. V Filonenko, V. V Sokolov, V.I. Chissov, E.A. Lukyanets, G.N. Vorozhtsov, Photodynamic therapy of early esophageal cancer., Photodiagnosis and Photodynamic Therapy. 5 (2008) 187–90.

[27] M. Fujiwara, K. Shiokawa, T. Kubota, Direct encapsulation of proteins into calcium silicate microparticles by water/oil/water interfacial reaction method and their responsive release behaviors, Materials Science and Engineering: C. 32 (2012) 2484–2490.

[28] M. Zeisser-Labouèbe, N. Lange, R. Gurny, F. Delie, Hypericin-loaded nanoparticles for the photodynamic treatment of ovarian cancer., Int. J. Pharm. 326 (2006) 174–81.

[29] C. Washington, Drug release from microdisperse systems: a critical review, Int. J. Pharm. 58 (1990) 1–12.

[30] A.-W. Xu, W.-F. Dong, M. Antonietti, H. Cölfen, Polymorph Switching of Calcium Carbonate Crystals by Polymer-Controlled Crystallization, Adv. Funct. Mater. 18 (2008) 1307–1313.

[31] S.K. Kim, M.B. Foote, L. Huang, Targeted delivery of EV peptide to tumor cell cytoplasm using lipid coated calcium carbonate nanoparticles., Cancer Letters. 334 (2013) 311–318.

[32] B.G. De Geest, S. De Koker, G.B. Sukhorukov, O. Kreft, W.J. Parak, A.G. Skirtach, et al., Polyelectrolyte microcapsules for biomedical applications, Soft Matter. 5 (2009) 282–291.

[33] C. Cortez, E. Tomaskovic-Crook, a. P.R. Johnston, B. Radt, S.H. Cody, a. M. Scott, et al., Targeting and Uptake of Multilayered Particles to Colorectal Cancer Cells, Adv. Mater. 18 (2006) 1998–2003.

[34] I. Tannock, D. Rotin, Acid pH in tumors and its potential for therapeutic exploitation, Cancer Research. (1989) 4373–4384.

[35] Y. Urano, D. Asanuma, Y. Hama, Y. Koyama, T. Barrett, M. Kamiya, et al., Selective molecular imaging of viable cancer cells with pH-activatable fluorescence probes., Nature Medicine. 15 (2009) 104–9.

[36] Y. Zhang, H.F. Chan, K.W. Leong, Advanced materials and processing for drug delivery: The past and the future., Adv. Drug Deliv. Rev. 65 (2013) 104–20.

Acknowledgements

Bogdan Parakhonskiy acknowledges funding by the Provincia autonoma di Trento (Marie Curie Actions, Trentino COFUND). Yulia Svenskaya acknowledges funding from the EU Erasmus Mundus Action 2 MULTIC Programme. Work was partially supported by RFBR, research projects № 12-03-33088 mol_a_ved.

List of figures

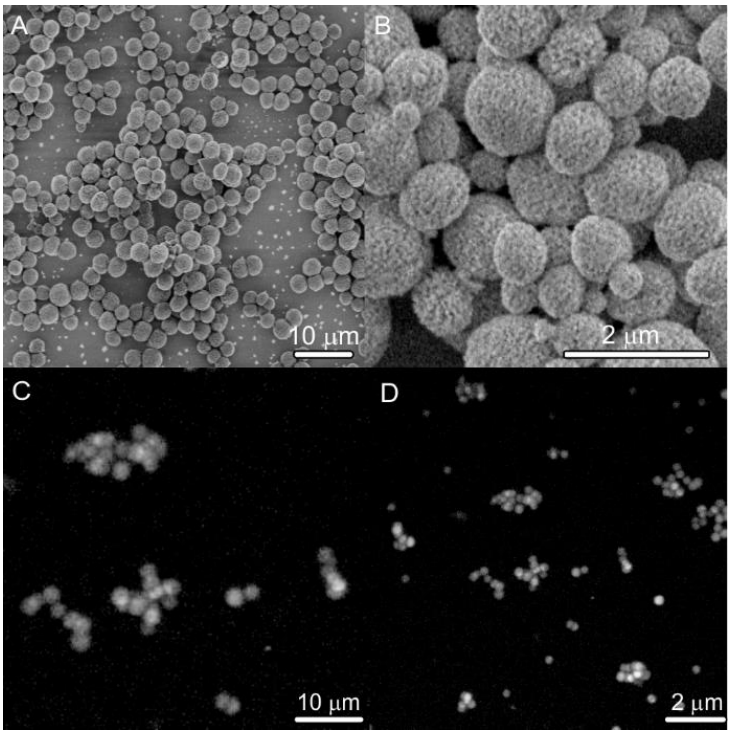

Fig. 1. Scanning electron microscopy images (A, B) and two-photon fluorescence images (C, D) of the calcium carbonate particles with average sizes of 3.6±0.5 μm (A, C) and 650±30 nm (B, D).

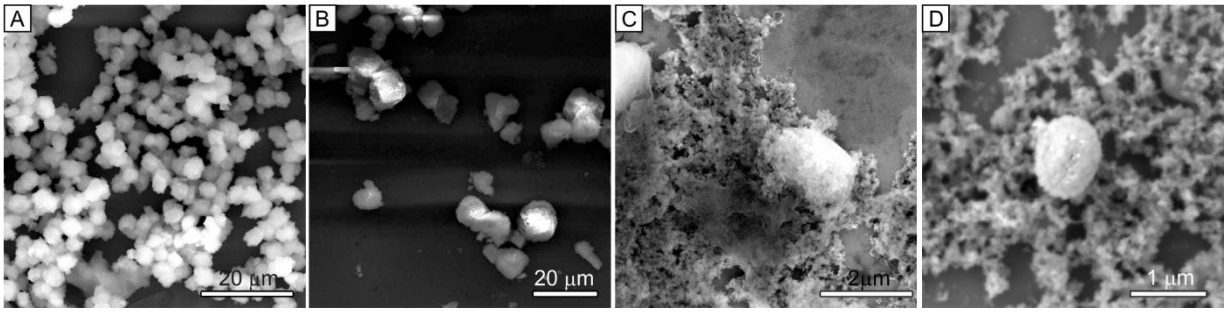

Fig. 2. Scanning electron microscopy images of big $CaCO_3$ particles in different crystal phases at different times: A) Mostly vaterite with a few calcite crystals, at day 3 after immersion in pH=7; B) Calcite crystals, at day 6 after immersion at pH=7.0; C) Mostly amorphous calcium carbonate and salts, 1h after immersion in pH=6.5. D) Mostly amorphous calcium carbonate and partially dissolved vaterite particles, at day 1 after immersion at pH=6.5.

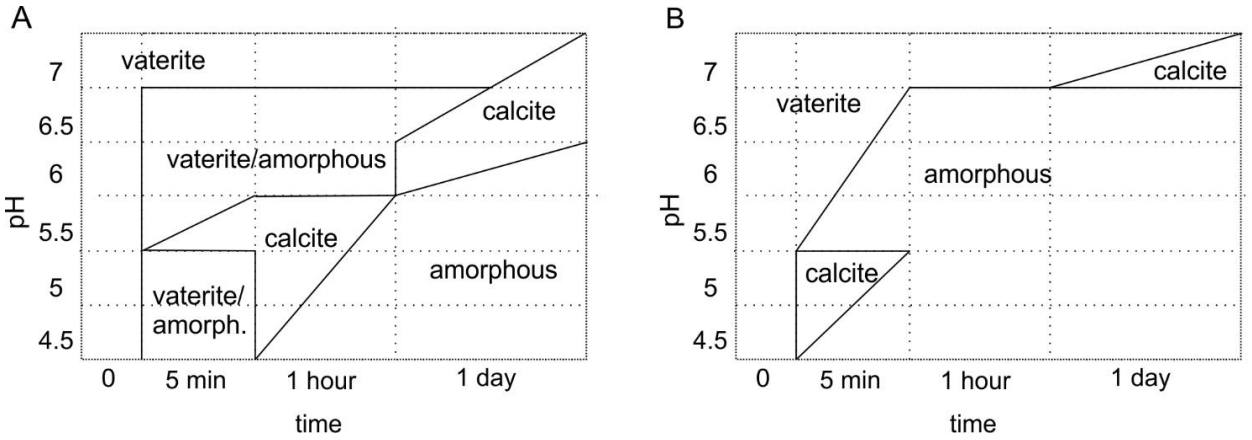

Figure 3. Phase-scheme of the loaded $CaCO_3$ particles at different pH during the 1st day. Big carriers are shown in scheme (A), small carriers in scheme (B).

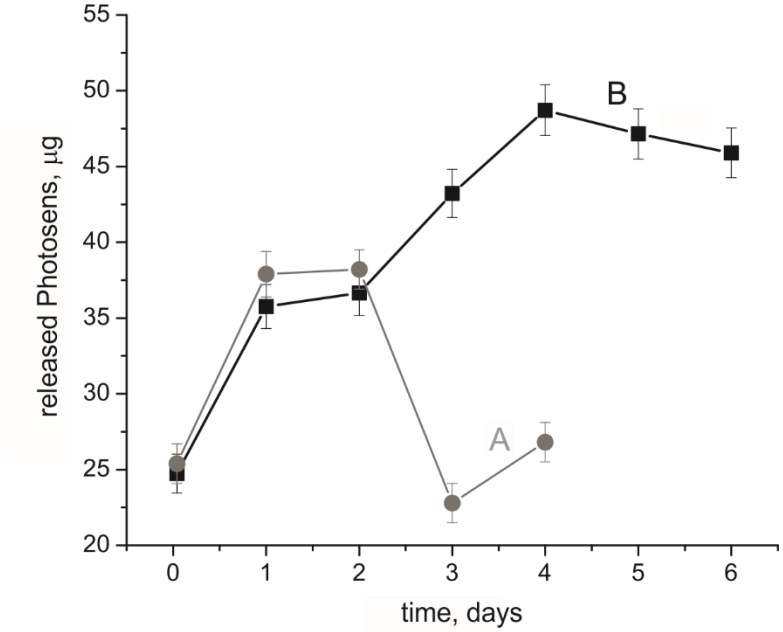

Fig. 4. Released amount of the Photosens in pH=7 buffer solution as a function of time for vaterite particles with different sizes: A) 3.6±0.5 µm and B) 650±30 nm. Curves show slower release and less re-adsorption for smaller carriers.